Received February 3, 2020, accepted March 8, 2020, date of publication March 16, 2020, date of current version March 26, 2020.

Digital Object Identifier 10.1109/ACCESS.2020.2981252

A New Method to Achieve Single-Polarization Guidance in Hollow-Core Negative-Curvature Fibers

SHIBO YAN[1], ZHENGGANG LIAN[2], SHUQIN LOU[1,3], XIN WANG[1], WAN ZHANG[1], AND ZIJUAN TANG[1]

[1]School of Electronic and Information Engineering, Beijing Jiaotong University, Beijing 100044, China
[2]Yangtze Optical Electronic Company Ltd., Wuhan 430205, China
[3]School of Electronic and Information Engineering, Hebei University of Technology, Tianjin 300130, China

Corresponding author: Shuqin Lou (shqlou@bjtu.edu.cn)

This work was supported in part by the National Natural Science Foundation of China under Grant 61775014, and in part by the key project of National Science Foundation of Hebei Province under Granted F2018202323.

ABSTRACT We propose a new method to achieve single-polarization guidance in a hollow-core negative-curvature fiber. Simulation results show that coating a layer of high-index material with a suitable thickness on the inner surface of one vertical cladding tube in a hollow-core negative-curvature fiber can effectively suppress *y*-polarized fundamental mode. Silicon is chosen as the high-index material in this paper. In the five-nested-tube silicon-coated negative-curvature fiber, the single-polarization region is located in the wavelength range of 1512–1587 nm with a broad bandwidth of 75 nm. The polarization extinction ratio is up to 1732 at the wavelength of 1550 nm. Moreover, the mode evolutions of *x*- and *y*-polarized fundamental modes in the five-nested-tube silicon-coated negative-curvature fiber are investigated to explain why *y*-polarized fundamental mode is suppressed. Compared with the traditional method of using different tube thicknesses to achieve single-polarization guidance in a negative-curvature fiber, this method possesses the advantages of broad single-polarization bandwidth and high error tolerance.

INDEX TERMS Hollow-core negative-curvature fiber, high polarization extinction ratio, single-polarization.

I. INTRODUCTION

Resonant-fiber-optic gyroscope (RFOG) is a potential candidate for high-performance inertial rotation sensors [1], [2]. Compared with the widely-used interferometric-fiber-optic gyroscopes, RFOGs ask for much shorter fiber length and possess advantages in size, weight, precision, and dynamic range [3], [4]. Optical ring resonator is one of the core elements in RFOGs that determine the accuracy of RFOGs. Various optical noise sources in optical ring resonators, such as Kerr effect and Rayleigh backscatter, restrict practical applications of RFOGs [5]. Using hollow-core fibers (HCFs) instead of conventional solid-core fibers in optical ring resonators can effectively reduce the above-mentioned optical noises and thermally induced nonreciprocity owing to guiding light in air cores [2], [6]. Polarization-maintaining fibers (PMFs), where two polarization states propagate with different propagation constants, are used in optical ring resonators to reduce polarization fading effects, but they also cause interference bias errors [7], [8]. Moreover, the temperature dependences of birefringence in PMFs decrease the stabilities of RFOGs. Using single-polarization fibers (SPFs) instead of PMFs can overcome these disadvantages [8]. Therefore, hollow-core single-polarization fibers that guide light in air cores with only one polarization state, are considered as one of the suitable candidates for the optical ring resonators in RFOGs. There have been some researches on single-polarization hollow-core photonic bandgap fibers (HCPBGFs). In 2014, Xu *et al*. proposed a single-polarization HCPBGF where two elliptical assistant holes were introduced into its cladding, and the polarization extinction ratio (PER) reached ∼4000 at the wavelength of 1550 nm [9]. In 2014, J. Fini *et al*. fabricated a 19-cell single-mode HCPBGF with two 7-cell shunts to suppress higher-order-modes where polarization dependence was produced by a tiny variation of the thickness of the core wall with angle, and the PER reached

The associate editor coordinating the review of this manuscript and approving it for publication was Rene Essiambre.

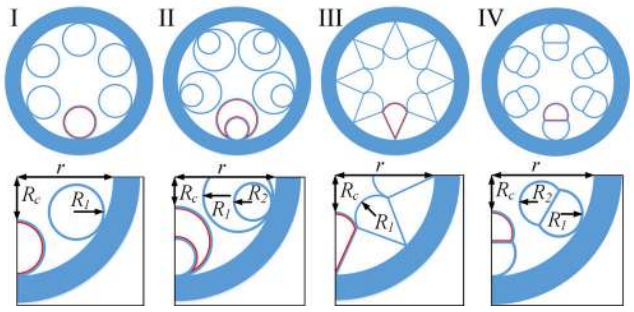

FIGURE 1. Four different kinds of NCFs with coated vertical tubes.

32 dB at 1532 nm [10]. In 2015, Serrão *et al.* showed a single-polarization HCPBGF with an asymmetric cladding structure, and the polarization dependent loss reached ∼800 dB/m at the wavelength of 1550 nm [11]. The cladding tubes in HCPBGFs are arranged strictly [12], which causes the complex structures of HCPBGFs. Moreover, a photonic bandgap only exists in the wavelength range near a specific wavelength, which causes the narrow transmission bandwidths of HCPBGFs [13].

A new type of HCF named negative-curvature fiber (NCF) recently attracts interest because of its attractive advantages, such as simple structure, broad transmission bandwidth, and flexible cladding design [14], [15]. There have been some previous researches on single-polarization NCFs. In 2018, Wei *et al*. proposed a single-polarization six-tube NCF, in which the PER reached 850 at the wavelength of 1550 nm [16]. In 2018, Yan *et al*. proposed a single-polarization double-ring NCF, in which the PER reached ∼17000 at the wavelength of 1550 nm [17].

Single-polarization transmissions in the above single-polarization NCFs are achieved by using different tubes thicknesses but this method is not suitable for broadband applications and difficult to achieve in a fabrication process due to narrow single-polarization bandwidth and high sensitivities to the thickness of thickened tubes. Here, we propose another method to get a single-polarization NCF that coating a layer of high-index material on the inner surface of one vertical cladding tube in an ordinary NCF. Silicon could be a candidate for this high-index material. This method possesses the advantages of broad single-polarization bandwidth and high error tolerance.

II. SINGLE-POLARIZATION GUIDANCE IN EXISTING NCFs

There have been various kinds of NCFs fabricated successfully. For example, six-tube NCF [18], five-nested-tube NCF [19], ice-cream NCF [20], and conjoined-cladding NCF. As shown in Fig. 1, four different kinds of NCFs are partially coated by high-index material, where blue region is silica glass and red region is the high-index material, and they are named as Fiber I, Fiber II, Fiber III, and Fiber IV, respectively. In this part, the core radii (R_c) and tube thicknesses (h_1) of these four NCFs are fixed at 12.5 μm and 0.5 μm, respectively; the thickness of the high-index material layer

TABLE 1. Structure parameters of four NCFs.

Fiber	R_c (μm)	h_1 (μm)	R_1/R_c	R_2/R_c	r (μm)
I	12.5	0.5	0.64	–	28.5
II	12.5	0.5	1.2	0.6	40
III	12.5	0.5	0.62	–	34.6
IV	12.5	0.5	0.75	0.7	38.1

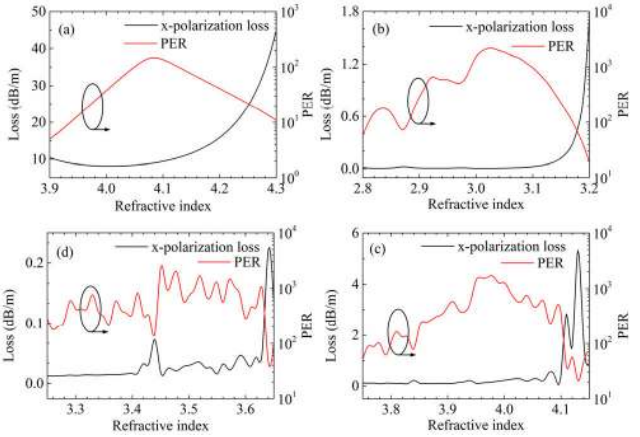

FIGURE 2. The x-polarization loss and PER as functions of refractive index of the high-index material at 1550 nm with a fixed h_2 of 100 nm in Fiber I (a), Fiber II (b), Fiber III (c), and Fiber IV (d).

is represented by h_2. The structure parameters are shown in Table. 1.

We first fix h_2 at 100 nm and then adjust the refractive index of high-index material. In this study, we use a finite-element method to analyze the characteristics of NCFs. The confinement loss is calculated by,

$$\text{Confinement Loss} = 8.686\frac{2\pi}{\lambda}\text{Im}\left(n_{eff}\right) \tag{1}$$

where λ is the wavelength, and n_{eff} is the effective refractive index. Here, PER is defined as the loss ratio of the y-polarized fundamental mode (FM) to the x-polarized FM. In this paper, single-polarization guidance can be determined if PER is higher than 100. Figure 2(a) to (d) display the x-polarization loss and PER as functions of the refractive index of the high-index material at 1550 nm in these four NCFs with a fixed h_2 of 100 nm. The PERs of Fiber I to IV can reach the maximum of 147, 2140, 1677, and 2320 when the refractive indexes are 4.08, 3.02, 3.98, and 3.45 with the x-polarization losses of 8.93 dB/m, 0.00577 dB/m, 0.161 dB/m, and 0.0189 dB/m at the wavelength of 1550 nm, respectively. Therefore, we can choose a suitable refractive index, i.e. a suitable material for a given h_2 to achieve single-polarization guidance in a NCF. Conversely, we can also choose a suitable h_2 for a given high-index material to achieve single-polarization guidance.

Silicon is a typical high-index material in near-infrared region. The refractive index of silicon is 3.48 at 1550 nm [21]. Moreover, the silicon-coated NCF has been fabricated

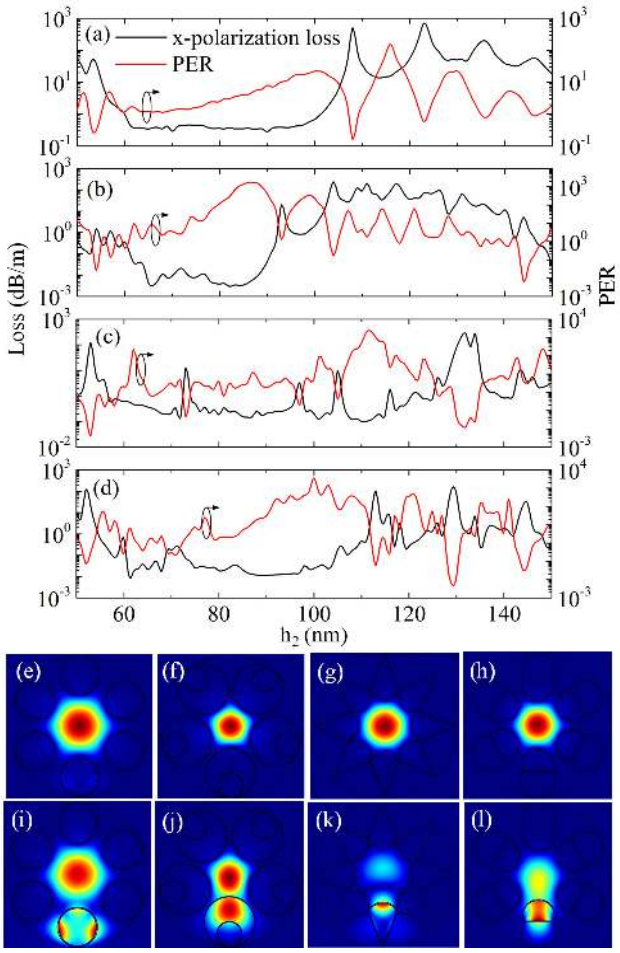

FIGURE 3. The x-polarization loss and PER as functions of h_2 at 1550 nm in Fiber I (a), Fiber II (b), Fiber III (c), and Fiber IV (d) and the mode field distributions of x-polarized FM in Fiber I (e), Fiber II (f), Fiber III (g), and Fiber IV (h) and y-polarized FM in Fiber I (i), Fiber II (j), Fiber III (k), and Fiber IV (k) at 1550 nm with the chosen h_2.

successfully by using a high-pressure chemical vapor deposition method in an existing NCF [22]. The process to obtain a partially silicon-coated NCF could be described as follows: first, the interfaces of a NCF are closed by using curing adhesives or other methods; second, the specific regions where we want to coat a layer of silicon are opened by using laser or electric discharge at two interfaces; finally, the silicon layer is deposited on the surfaces of the specific regions in the processed NCF by using a high-pressure chemical vapor deposition method. One of the significant advantages of RFOG is the short fiber length. The needed fiber length of RFOG is usually several meters. Although the length of the fabricated silicon-coated NCF is not very long, it is promising to meet the demands of RFOG with the improvement of fabrication technology and the development of RFOG technology. The intrinsic absorption of silicon is quite low at 1550 nm [23]. Therefore, silicon is a suitable candidate for the high-index material in our designs. In the following part, silicon is chosen as the high-index material to analyze.

Figure 3(a) to (d) display the x-polarization loss and PER as functions of h_2 at 1550 nm in these four NCFs. The PERs of Fiber I to IV can reach the maximum of 154, 1732, 2192, and 3646 when h_2 is 116 nm, 86 nm, 112 nm, and 100 nm at 1550 nm, respectively. Therefore, 116 nm, 86 nm, 112 nm, and 100 nm are chosen as the values of h_2 in Fiber I to IV, respectively. Figure 3(e) to (h) respectively shows the mode field distributions of the x-polarization at 1550 nm in Fiber I to IV with the chosen h_2 and Fig. 3(i) to (l) respectively show those of y-polarization at 1550 nm. It can be seen that y-polarization states in these four NCFs couple into the silicon-coated tubes while x-polarization states do not, and thus single-polarization guidance is achieved in these four NCFs. Moreover, the error tolerance of h_2 to maintain single-polarization guidance in Fiber I to IV is 1%, 12%, 8%, and 12%. The material absorption of silicon layer is neglected because of the low intrinsic absorption of silicon at 1550 nm, and extremely low energy fraction of the silicon layer. Although y-polarized FM couples to the silicon-coated tube, only a little energy existing in the silicon layer. For example, in Fiber II, the energy fractions of the silicon layer are respectively 0.0007% and 0.046% for x-polarized FM and y-polarized FM and those of core region are respectively 99.3% and 54.0% for x- and y-polarized FMs. We have calculated the material absorption of the silicon layer in Fiber II. The material absorption losses of the silicon layer are 3.94×10^{-11} dB/m and 1.94×10^{-11} dB/m in x-polarized FM and y-polarized FM at 1550 nm, respectively. The material absorption losses of the silicon layer are much lower than the confinement losses of FMs. Therefore, it is reasonable to neglect the material absorption loss of the silicon layer. Furthermore, we notice that h_2 needs a lower value for a higher refractive index of high-index material in a specific NCF and vice versa. This phenomenon is explained in the latter part.

Figure 4(a) to (d) display the x-polarization loss and PER as functions of wavelength in Fiber I to IV, respectively. In Fiber I, the single-polarization region is located in the wavelength range of 1547–1554 nm; the single-polarization bandwidth is 7 nm; the highest PER is 159 at the wavelength of 1552 nm with the x-polarization loss of 15 dB/m; the x-polarization loss and PER at 1550 nm are 15.8 dB/m and 154, respectively. In Fiber II, the single-polarization region is located in the wavelength range of 1512–1587 nm; the single-polarization bandwidth is up to 75 nm; the highest PER is 1813 at the wavelength of 1551 nm with the x-polarization loss of 0.0041 dB/m; the x-polarization loss and PER at 1550 nm are 0.0044 dB/m and 1732, respectively. In Fiber III, the single-polarization region is located in the wavelength range of 1532–1562 nm; the single-polarization bandwidth is up to 30 nm; the highest PER is 2192 at the wavelength of 1550 nm with the x-polarization loss of 0.11 dB/m. In Fiber IV, the single-polarization region is located in the wavelength range of 1509–1586 nm; the single-polarization bandwidth is up to 77 nm; the highest PER is 17715 at the wavelength of 1574 nm with the x-polarization loss of 0.0082 dB/m; the x-polarization loss and PER at 1550 nm are 0.024 dB/m and 3646, respectively. Following the above

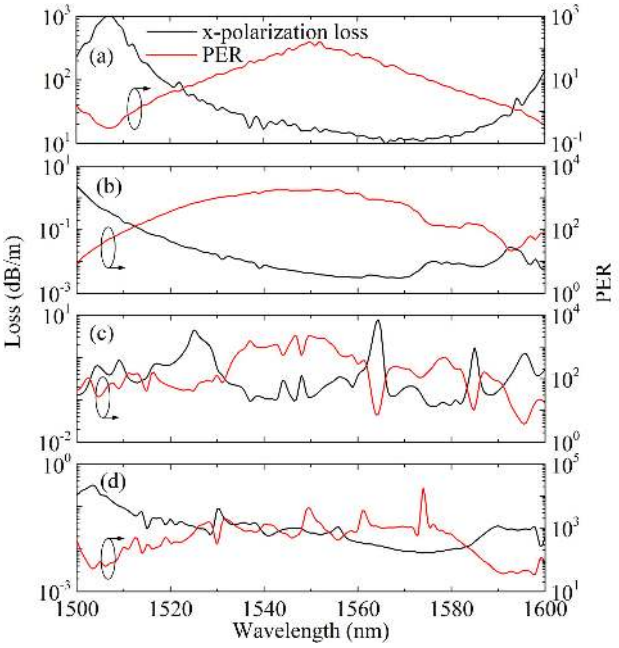

FIGURE 4. The x-polarization loss and PER as functions of wavelength in Fiber I (a), Fiber II (b), Fiber III (c), and Fiber IV (d).

discussion, we achieve single-polarization guidance in different kinds of NCFs by coating a layer of silicon. The single-polarization performance in Fiber I is the worst due to the high loss of this kind of single-ring NCF. Nested and nodeless structures have been considered as effective designs for low loss NCFs. In other NCFs, this method shows the advantages of broad single-polarization bandwidth and high error tolerance of silicon layer thickness.

Nested NCFs have been considered as effective designs of low-loss NCFs, and have been fabricated successfully [15], [19], [24]. Therefore, we take the above-mentioned five-nested-tube NCF, i.e. Fiber II, as an instance to analyze the single-polarization characteristics in the next section.

III. DETAILED ANALYSIS OF FIVE-NESTED-TUBE NCF

We first analyze the mode evolutions of x- and y-polarized FMs in five-nested-tube NCF. The structure parameters are as shown in Table. 1 and h_2 is chosen as 86 nm. Figure 5(a) and (b) display the effective refractive indexes and losses of x-polarization mode, y-polarization odd mode (y_{odd}-polarization) and y-polarization even mode (y_{even}-polarization) in the wavelength of 1500–1600 nm, respectively. Figure 5(c) displays the mode field distributions of these modes at 1500, 1525, 1550, 1575, and 1600 nm. Seen in the mode field distributions at 1550 nm, the y_{odd}-polarization, in which the polarization directions of the core region and silicon-coated tube region are opposite, and y_{even}-polarization in which the polarization directions of core region and silicon-coated tube region are same, are formed due to the mode couple between y-polarization core mode and the mode existing in the silicon-coated tube region which is named as cladding mode (CM) in this paper.

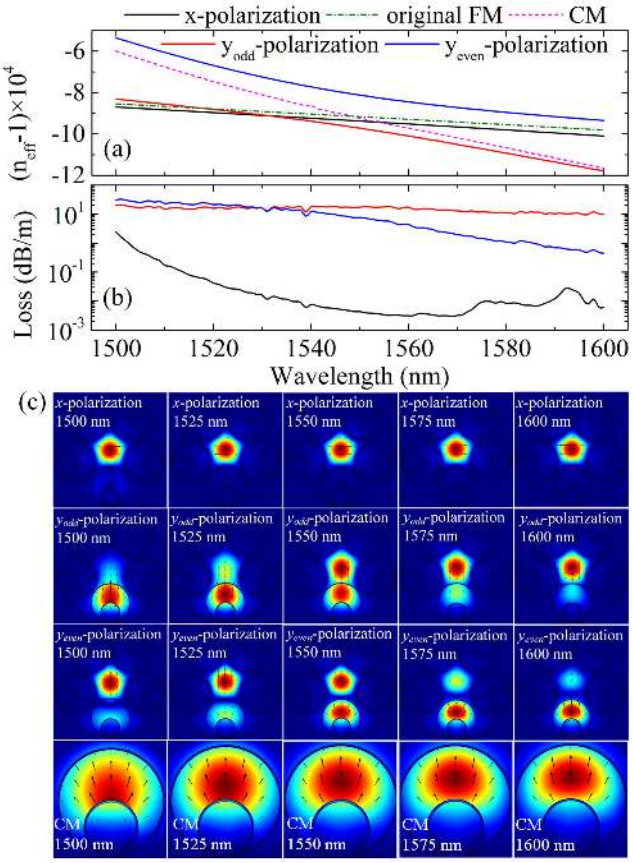

FIGURE 5. Effective refractive indexes (a) of x-polarization, y_{odd}-polarization and y_{even}-polarization mode, CM and original FM, and losses (b) of x-polarization, y_{odd}– polarization and y_{even}-polarization mode in the wavelength of 1500–1600 nm and mode evolution of these modes (c).

To investigate the reason why single-polarization guidance is achieved, we retain the silicon-coated tube only and analyze CM. The dashed line in Fig. 5(a) represents the refractive index of CM and the dot-dash line represents the refractive index of original FM which is the FM in the five-nested-tube NCF without silicon layer. It can be seen that they are crossed around the wavelength of 1550 nm. Therefore, the refractive index of original y-polarization, which is the y-polarized FM in the NCF without silicon layer, is close to that of CM at 1550 nm, and y_{odd}-polarization and y_{even}-polarization are formed due to the anti-crossing effect in the mode couple between original y-polarization and CM at 1550 nm. With a decrease of wavelength, y_{odd}-polarization gradually gets closer to CM in short wavelength region, and y_{even}-polarization dose with an increase of wavelength in long-wavelength region. The x-polarization doesn't couple with CM because their polarized directions are not matched although their effective refractive indexes are also approximately equal at 1550 nm. This is the reason why the phenomenon that only y-polarization couples into silicon-coated tubes appears. In this paper, the lower loss of y_{odd}-polarization and y_{even}-polarization is chosen to calculate PER.

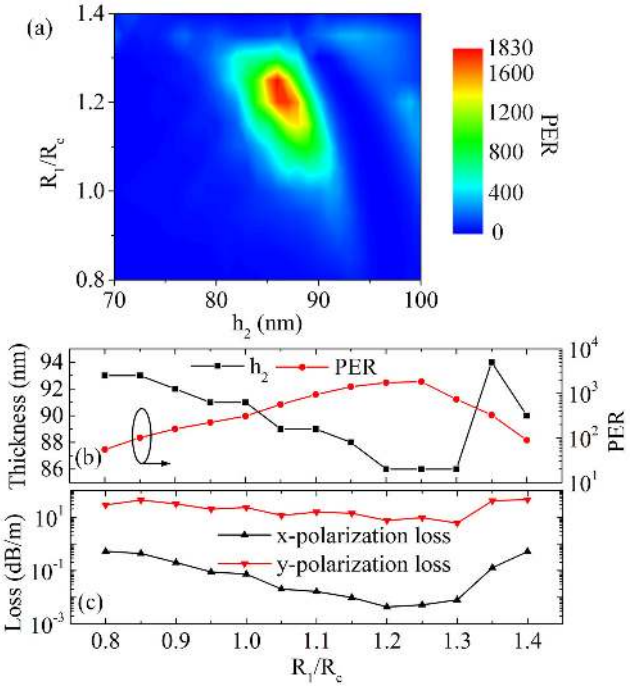

FIGURE 6. The PER as functions of h_2 and R_1/R_c with a fixed R_c of 12.5 μm at 1550 nm (a). The h_2 which can reach the maximum PER and the maximum PER for different R_1/R_c at 1550 nm (b) and the losses of x-polarization and y-polarization for those cases (c).

We have found that the effective refractive index of CM increases with an increase of the refractive index of high-index material and layer thickness. To keep mode couple, the refractive index of CM should be kept almost unchanged. This explains why h_2 needs a lower value for a higher refractive index of high-index material. We focus on adjusting parameters to tune the y-polarization into resonance for single x-polarization guidance in this paper. In fact, the x-polarization can also couple with a certain CM under a suitable h_2, which can realize single y-polarization guidance. This is the reason for the appearance of some loss peaks of x-polarization in Fig. 3.

The silicon layer brings a high birefringence between y-polarized CM and x-polarized CM. The CM in Fig. 5(c) is the y-polarized CM. The effective refractive index of y-polarized CM is 0.99908 at 1550 nm, while that of x-polarized CM is 0.99868. Therefore, x-polarization doesn't couple with x-polarized CM when y-polarization couples with y-polarized CM because of a large difference in mode effective refractive index between x-polarization and x-polarized CM. This explains why the silicon layer is essential. If there is no silicon layer, the birefringence of y-polarized CM and x-polarized CM will be very small and the mode couples between FM and the CM with the same polarization direction will occur at the same time, which eliminates single-polarization guidance.

Then we analyze the relationship between h_2 and R_1. Figure 6(a) displays the PER as functions of h_2 and R_1/R_c at 1550 nm. The other structure parameters are as shown in Table. 1. The PER can maintain a high value in a large range of h_2 and R_1/R_c. PER can keep higher than 100 in the h_2 range of 80 to 91 nm with R_1/R_c of 1.2 and in the R_1/R_c range of 0.9 to 1.25 with h_2 of 90 nm. Therefore, this design possesses a high error tolerance of the thickness of silicon layer and large cladding tube size. Figure 6(b) displays the h_2 which can reach the maximum PER and the maximum PER for different R_1/R_c at 1550 nm. Figure 6(c) displays the losses of x-polarization and y-polarization for those cases. The maximum PER is 1827 when R_1/R_c is 1.25 and h_2 is 86 nm. The needed h_2 to achieve the maximum PER experiences a downward trend and x-polarization loss decreases with an increase of R_1/R_c until R_1/R_c reaches 1.25. This is because the effective refractive index of CM increases with an increase of R_1, and thus the needed h_2 decreases to keep mode couple. When R_1/R_c increases to 1.25, the FM in air core starts to couple into the region between the large cladding tubes and their nested small tubes because of the large size of this region and thus the losses of x-polarization and y-polarization both increase with an increase of R_1/R_c.

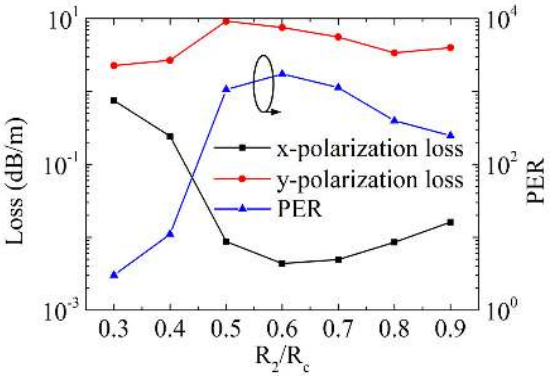

FIGURE 7. The losses of x-polarization and y-polarization and PER as functions of R_2/R_c with R_1/R_c of 1.2 and h_2 of 86 nm at 1550 nm.

Figure 7 displays the losses of x-polarization and y-polarization and PER as functions of R_2/R_c with R_1/R_c of 1.2 and h_2 of 86 nm at 1550 nm. The x-polarization losses decrease firstly and then increase with an increase of R_2/R_c. The PER reaches the maximum of 1732 when R_2/R_c is 0.6 and decreases when R_2/R_c is changed from 0.6. This is because the effective refractive index of CM changes with a change of R_2/R_c from 0.6, which weakens the mode couple between CM and y-polarization. PER can keep > 100 with R_2/R_c varying in 0.5 to 0.9.

Then we analyze the relationship between h_2 and core radius. Figure 8 displays the PER as functions of h_2 and R_c/R_o at 1550 nm. R_o is the original core radius of 12.5 μm. The other structure parameters are as shown in Table. 1. The PER can maintain a high value in a large range of h_2 and R_c/R_o. Figure 8(b) displays the h_2 which can reach the maximum PER and the maximum PER for different R_c/R_o at 1550 nm. Figure 8(c) displays the losses of x-polarization and y-polarization for those cases. The needed h_2 changes slightly with an increase of R_c/R_o. This is because the effective

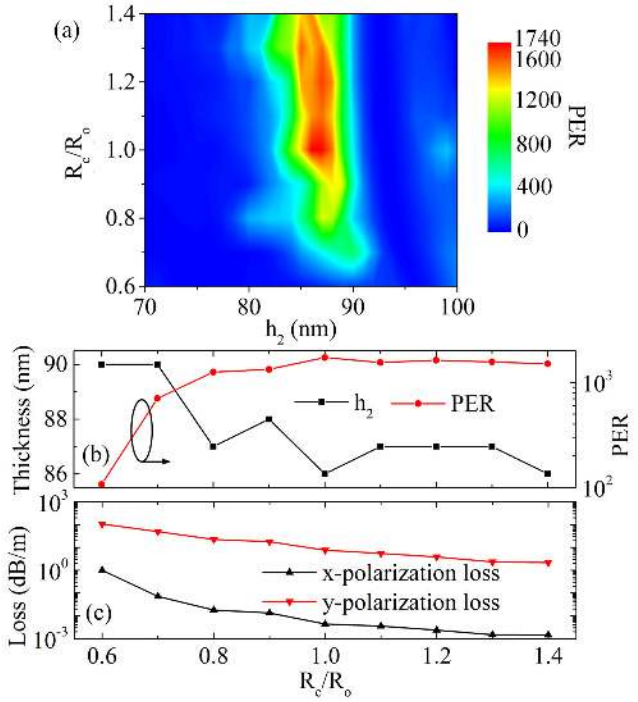

FIGURE 8. PER as functions of h_2 and R_c/R_o at 1550 nm (a). The h_2 which can reach the maximum PER and the maximum PER for different R_c/R_o at 1550 nm (b) and the losses of x-polarization and y-polarization for those cases (c).

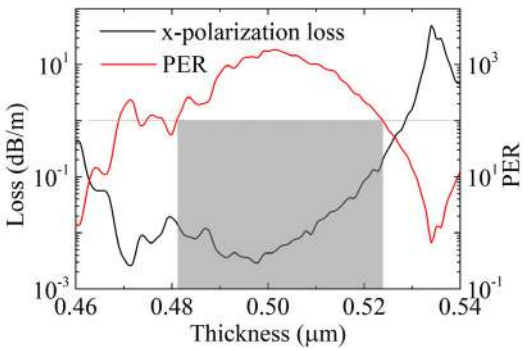

FIGURE 9. The x-polarization loss and PER as functions of h_1 at 1550 nm.

refractive indexes of FM in air core and CM both increase and keep approximating to each other with an increase of R_c/R_o. The PER can keep higher than 100 in the h_2 range of 79 to 90 nm with R_c/R_o of 1.2 and the R_c/R_o range of 0.6 to 1.4 with h_2 of 90 nm. Therefore, this design possesses a high error tolerance of the core radius.

The transmission characteristics of NCFs are influenced by tube thickness. In the fabrication process of NCFs, tube thickness may deviate from the expected value. Therefore, we investigate the influence of tube thickness on single-polarization performance in this NCF. Figure 9 displays the x-polarization loss and PER as functions of h_1. The other structure parameters are as shown in Table. 1. PER can keep higher than 100 in the thickness range of 0.481 to 0.522 μm, which confirms that the error tolerance of tube thickness is $\sim \pm 4\%$.

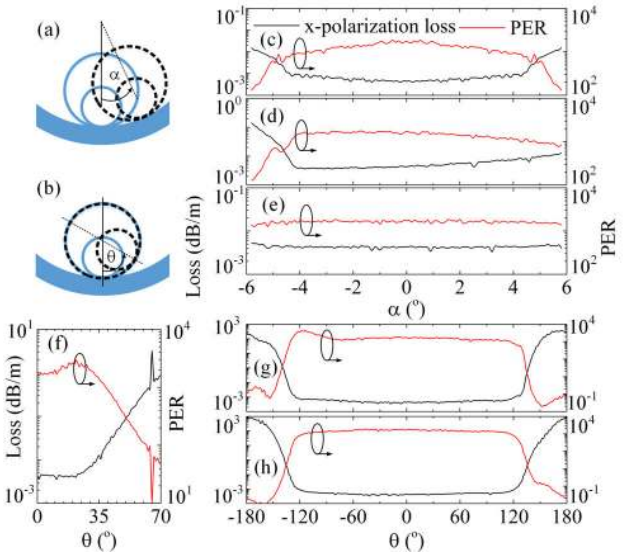

FIGURE 10. Rotation of a cladding tube around fiber center (a) and its own center (b). The x-polarization loss and PER at 1550 nm as functions of α with rotating tube 1 (c), tube 2 (d), and tube 3 (e), and as functions of θ with rotating tube 1 (f), tube 2 (g), and tube 3 (h).

In the fabrication process of this kind of nested NCF, the rotation of cladding tubes usually happens. Therefore, we investigate the influence of the rotation of cladding tubes on single-polarization performance. To simplify the analysis, we discuss the conditions that one cladding tube rotates in different positions. The silicon-coated tube is marked as tube1; the cladding tube adjacent to the silicon-coated tube is marked as tube 2; the cladding tube alternate with the silicon-coated tube is marked as tube 3. Figure 10 displays two kinds of rotating cladding tubes and single-polarization performance with one rotating cladding tube. The α and θ are the rotation angle of a cladding tube around the center of fiber and itself, respectively. Due to the geometry parameters, the maximum value of α is 5.8°. Figure 10(c) to (e) and (f) to (h) display the x-polarization loss and PER at 1500 nm with rotating tube 1 to 3 around the center of fiber and itself, respectively. PER keep higher than 100 with α varied in the range of $-5.8°$ to $+5.8°$. The angle range of θ keeping PER $>$ 100 is $-61°$ to $+61°$ for tube 1, $-136°$ to $+132°$ for tube 2, and $-130°$ to $+130°$ for tube 3. Therefore, this fiber possesses a high tolerance of rotating cladding tubes.

In this paper, silicon is chosen as the high-index material to achieve single-polarization guidance. However, there are some kinds of monatomic silicon, such as monocrystalline silicon, polycrystalline silicon, and amorphous silicon, with a slight difference in refractive indexes. Moreover, refractive indexes of silicon vary with temperature. In Ref. [22], the high-index layer is consisted by amorphous hydrogenated silicon with a refractive index of $\sim$3.6. Therefore, we investigate the influence of the refractive index on single-polarization performance. Figure 11 displays the x-polarization loss and PER as functions of the refractive index of the silicon layer at 1550 nm. The refractive index of silicon layer varying

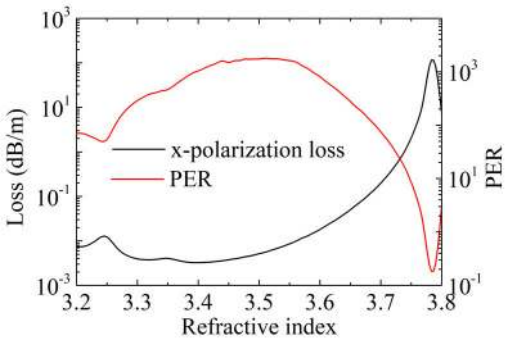

FIGURE 11. The x-polarization loss and PER as of the refractive index of the silicon layer at 1550 nm.

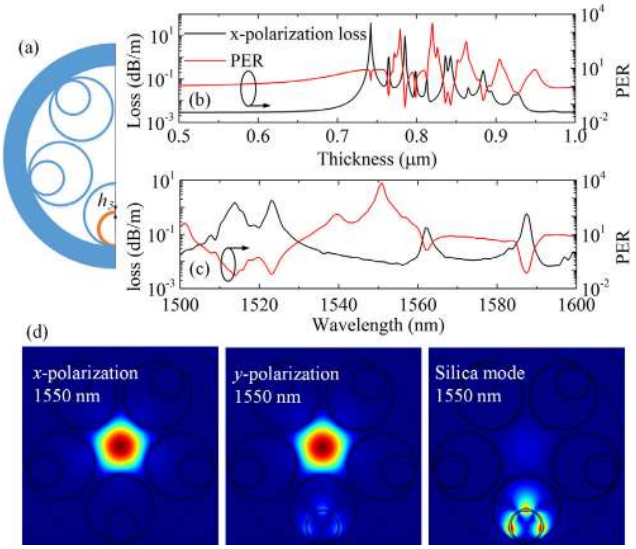

FIGURE 12. Cross section of the five-nested-tube NCF with thickened tube (a). The x-polarization loss and PER as functions of h_3 at 1550 nm (b) and the x-polarization loss and PER as functions of wavelength with h_3 of 0.82 μm (c) and the mode field distributions of x-polarization, y-polarization, and silica mode with h_3 of 0.82 μm at 1550 nm (d).

in 3.27 to 3.69 can keep PER $>$ 100 at 1550 nm. In fact, as discussed in the earlier part, if there is a more suitable candidate for high-index material, we can use it to obtain similar single-polarization performance by adjusting h_2 to a suitable value.

IV. COMPARISON WITH TRADITIONAL METHOD

The traditional method to achieve single-polarization guidance in NCFs is using different tube thicknesses [16], [17]. However, this method has some disadvantages such as narrow single-polarization bandwidth and high sensitivities to tube thickness. For direct comparison, we apply this method in the same five-nested-tube NCF whose structure parameters are as shown in Table 1. The cross section of this NCF is shown in Fig. 12(a). The thickened wall thickness is represented by h_3. Figure 12(b) displays the x-polarization loss and PER as functions of h_3 at 1550 nm. PER reaches the maximum of 3075 when h_3 is 0.82 μm, and can keep higher than 100 in the h_3 range of 0.817 μm to 0.822 μm. The error tolerance of h_3 is only 0.6%, which is very difficult to achieve in the fabrication process. Figure 12(c) displays the x-polarization and PER as functions of wavelength with h_3 of 0.82 μm. The single-polarization bandwidth is 9 nm in the wavelength range of 1546–1555 nm. Figure 12(d) displays the mode field distributions of x-polarization, y-polarization, and the mode surrounding the thickened tube which is called silica mode. Silica mode couples with y-polarization and thus single-polarization guidance is achieved. However, the effective refractive index of silica mode varies considerably with changes of thickened thicknesses or wavelengths. Therefore, this method has the disadvantages of narrow single-polarization bandwidth and high sensitivities to thickened thicknesses. Compared with the traditional design with different tube thicknesses, our design has huge advantages in single-polarization bandwidth and error tolerance of structure parameters. It provides a new design thought for single-polarization NCFs.

V. CONCLUSION

In conclusion, we propose a method to achieve single-polarization guidance in different kinds of NCFs that coating a layer of high-index material in one vertical cladding tube and explain the single-polarization mechanism. The simulation results of single-polarization five-nested-tube NCF confirm that this method possesses the advantages of broad single-polarization bandwidth and high error tolerance of structure parameters compared with the traditional method of using different tube thicknesses. This method is more for practical conditions and has the potential to be applied in RFOGs and other applications, in which single-polarization HCFs are needed.

REFERENCES

[1] R. E. Meyer, S. Ezekiel, D. W. Stowe, and V. J. Tekippe, "Passive fiber-optic ring resonator for rotation sensing," *Opt. Lett.*, vol. 8, no. 12, pp. 644–646, Dec. 1983.
[2] M. A. Terrel, M. J. F. Digonnet, and S. Fan, "Resonant fiber optic gyroscope using an air-core fiber," *J. Lightw. Technol.*, vol. 30, no. 7, pp. 931–937, Apr. 2012.
[3] Z. Jin, X. Yu, and H. Ma, "Closed-loop resonant fiber optic gyro with an improved digital serrodyne modulation," *Opt. Express*, vol. 21, pp. 26578–26588, Nov. 2013.
[4] Z. Jin, X. Yu, and H. Ma, "Resonator fiber optic gyro employing a semiconductor laser," *Appl. Opt.*, vol. 51, no. 15, pp. 2856–2864, May 2012.
[5] D. Ying, M. S. Demokan, X. Zhang, and W. Jin, "Analysis of kerr effect in resonator fiber optic gyros with triangular wave phase modulation," *Appl. Opt.*, vol. 49, no. 3, pp. 529–535, Jan. 2010.
[6] G. A. Sanders, L. K. Strandjord, and T. Qiu, "Hollow core fiber optic ring resonator for rotation sensing," in *Proc. Opt. Fiber Sensors*, Cancun, Mexico, 2006, pp. 1–4, Paper ME6.
[7] L. K. Strandjord and G. A. Sanders, "Performance improvements of a polarization-rotating resonator fiber optic gyroscope," *Proc. SPIE*, vol. 1795, pp. 94–105, Mar. 1993.
[8] Y. Yan, H. Ma, and Z. Jin, "Reducing polarization-fluctuation induced drift in resonant fiber optic gyro by using single-polarization fiber," *Opt. Express*, vol. 23, pp. 2002–2009, Feb. 2015.
[9] D. J. Xu, H. R. Song, and W. Wang, "Analysis of transmission characteristic in single polarization dual elliptical assistant holes hollow fiber," *Appl. Mech. Mater.*, vols. 475–476, pp. 1359–1362, Dec. 2013.
[10] J. M. Fini, J. W. Nicholson, B. Mangan, L. Meng, R. S. Windeler, E. M. Monberg, A. DeSantolo, F. V. DiMarcello, and K. Mukasa, "Polarization maintaining single-mode low-loss hollow-core fibres," *Nature Commun.*, vol. 5, no. 1, p. 5085, Dec. 2014.

[11] V. A. Serrão and M. A. R. Franco, "Single-polarization single-mode hollow core photonic bandgap fiber for gyroscope applications," in *Proc. 24th Int. Conf. Opt. Fibre Sensors*, Sep. 2015, Art. no. 963470.
[12] R. F. Cregan, "Single-mode photonic band gap guidance of light in air," *Science*, vol. 285, no. 5433, pp. 1537–1539, Sep. 1999.
[13] S. A. Mousavi, S. R. Sandoghchi, D. J. Richardson, and F. Poletti, "Broadband high birefringence and polarizing hollow core antiresonant fibers," *Opt. Express*, vol. 24, pp. 22943–22958, Oct. 2016.
[14] S. Yan, S. Lou, X. Wang, T. Zhao, and W. Zhang, "High-birefringence hollow-core anti-resonant THz fiber," *Opt. Quantum Electron.*, vol. 50, no. 3, p. 162, Mar. 2018.
[15] C. Wei, R. Joseph Weiblen, C. R. Menyuk, and J. Hu, "Negative curvature fibers," *Adv. Opt. Photon.*, vol. 9, no. 3, pp. 504–561, Sep. 2017.
[16] C. Wei, C. R. Menyuk, and J. Hu, "Polarization-filtering and polarization-maintaining low-loss negative curvature fibers," *Opt. Express*, vol. 26, pp. 9528–9540, Apr. 2018.
[17] S. Yan, S. Lou, W. Zhang, and Z. Lian, "Single-polarization single-mode double-ring hollow-core anti-resonant fiber," *Opt. Express*, vol. 26, pp. 31160–31171, Nov. 2018.
[18] P. Uebel, M. C. Günendi, M. H. Frosz, G. Ahmed, N. N. Edavalath, J.-M. Ménard, and P. S. J. Russell, "Broadband robustly single-mode hollow-core PCF by resonant filtering of higher-order modes," *Opt. Lett.*, vol. 41, no. 9, pp. 1961–1964, May 2016.
[19] A. F. Kosolapov, G. K. Alagashev, A. N. Kolyadin, A. D. Pryamikov, A. S. Biryukov, I. A. Bufetov, and E. M. Dianov, "Hollow-core revolver fibre with a double-capillary reflective cladding," *Quantum Electron.*, vol. 46, no. 3, pp. 267–270, Mar. 2016.
[20] B. Sherlock, F. Yu, J. Stone, S. Warren, C. Paterson, M. A. A. Neil, P. M. W. French, J. Knight, and C. Dunsby, "Tunable fibre-coupled multiphoton microscopy with a negative curvature fibre," *J. Biophoton.*, vol. 9, no. 7, pp. 715–720, Jul. 2016.
[21] H. H. Li, "Refractive index of silicon and germanium and its wavelength and temperature derivatives," *J. Phys. Chem. Reference Data*, vol. 9, no. 3, pp. 561–658, Jul. 1980.
[22] W. Belardi, F. De Lucia, F. Poletti, and P. J. Sazio, "Composite material hollow antiresonant fibers," *Opt. Lett.*, vol. 42, no. 13, pp. 2535–2538, Jul. 2017.
[23] J. Degallaix, R. Flaminio, D. Forest, M. Granata, C. Michel, L. Pinard, T. Bertrand, and G. Cagnoli, "Bulk optical absorption of high resistivity silicon at 1550 nm," *Opt. Lett.*, vol. 38, no. 12, pp. 2047–2049, Jun. 2013.
[24] T. Bradley, J. Hayes, Y. Chen, G. Jasion, S. R. Sandoghchi, and R. Slavík, "Record low-loss 1.3 dB/km data transmitting antiresonant hollow core fibre," in *Proc. Eur. Conf. Opt. Commun. (ECOC)*, Sep. 2018, pp. 1–3.

SHIBO YAN was born in Liaoning, China, in 1992. He received the B.S. degree from Beijing Jiaotong University, Beijing, China, in 2015, where he is currently pursuing the Ph.D. degree in communication and information engineering. His current research interests include hollow core antiresonant fiber, terahertz waveguide, and so on.

ZHENGGANG LIAN received the bachelor's and Ph.D. degrees in electronic engineering from the University of Nottingham, in 2006 and 2010, respectively. He was with the Optoelectronics Research Centre, University of Southampton. Since 2014, he has been with Yangtze Optical and Electronics Company Ltd., Wuhan, and oversee the Research and Development Department. In 2016, he joined the Huazhong University of Science and Technology, as a Part-Time Professor. He has generated more than 60 publications. He holds over 16 patents. His research interests include design and fabrication of speciality optical fibers and targeting application, include optoelectronic sensing, IR transmission, and high power fiber lasers.

SHUQIN LOU received the Ph.D. degree from Beijing Jiaotong University, Beijing, China, in 2005. She is currently a Professor with the School of Electronic and Information Engineering, Beijing Jiaotong University. She has authored or coauthored more than 200 articles in the international journals, including *Optics Express*, the IEEE Photonics Technology Letters, the IEEE/OSA Journal of Lightwave Technology, and so on. Her current research interests include microstructured fiber, fiber components, fiber laser, and fiber sensor.

XIN WANG received the Ph.D. degree from Beijing Jiaotong University, Beijing, China, in 2016. She is currently an Associate Professor with the School of Electronic and Information Engineering, Beijing Jiaotong University. She has authored or coauthored more than 20 articles in the international journals, including the IEEE Journal of Selected Topics in Quantum Electronics, the IEEE Photonics Journal, *Applied Optics*, and so on. Her research interests include microstructured fiber, fiber property, and fabrication.

WAN ZHANG received the B.S. and M.S. degrees in communication and information system from Yanshan University, Qinhuangdao, China, in 2012 and 2015, respectively. She is currently pursuing the Ph.D. degree in communication and information system with Beijing Jiaotong University, Beijing, China. Her research interests include microstructured fiber, hollow core antiresonant fiber, fiber sensor, and surface plasmon resonance.

ZIJUAN TANG was born in Shanxi, China, in 1993. She received the bachelor's degree from the School of Electronic and Information Engineering, Beijing Jiaotong University, Beijing, China, in 2016, where she is currently pursuing the Ph.D. degree in communication and information system. Her research interests include fiber sensors and lasers based on special fibers.